



Captides: rigid junctions between beta sheets and small molecules

Brandon L. Kier* and Niels H. Andersen

An extensive series of covalently linked small molecule-peptide adducts based on a terminally capped-beta hairpin motif is reported. The constructs can be prepared by standard solid-phase Fmoc chemistry with one to four peptide chains linked to small molecule hubs bearing carboxylic acid moieties. The key feature of interest is the precise, buried environment of the small molecule, and its rigid orientation relative to one or more short but fully structured peptide chain(s). Most of this study employs a minimalist nine residue 'captide', a capped β -turn, but we illustrate general applicability to peptides which can terminate in a beta strand. The non-peptide portion of these adducts can include nearly any molecule bearing one or more carboxylic acid groups. Fold-dependent rigidity sets this strategy apart from the currently available bioconjugation methods, which typically engender significant flexibility between peptide and tag. Applications to catalyst enhancement, drug design, higher-order assembly, and FRET calibration rulers are discussed. Copyright © 2014 European Peptide Society and John Wiley & Sons, Ltd.

Additional supporting information may be found in the online version of this article at the publisher's web site.

Keywords: bioconjugation; beta hairpins; preorganization; structure design; fold stabilization; on-resin methods

Introduction

Hybrid small molecule/peptide constructs represent a large class of bioconjugates. They frequently take the form of peptides with unnatural amino acids in the chain, most commonly as functionalized Asp, Glu, Lys, or especially Cys residues. Peptide/small molecule adducts are made for a variety of reasons including protease-resistance [1–4], improved delivery to cells [5–9], catalysis [8–13], fluorescent signaling, and to improve binding affinity [14–16].

Small molecule attachment to a sidechain, or to the *N*-terminus via a flexible linker, results in flexible species in which there is not a single defined stereochemical relationship between the peptide unit and the appended molecule. Further, such adducts have rarely been based on structured peptide folds. Covalent dimers and higher-order oligomers are less common. These are typically multimers of solution-unstructured peptides [17–19] held together via floppy linkers, e.g., alkyl di-acids [20,21], PEG (polyethylene glycol) [16,21–23], lysine/lysine multiple attachment peptides [24–28], bis-maleimides [29], or a simple disulfide. The novelty of our current approach stems from the innate rigidity of the scaffolds – a result of combining low-flexibility hubs with designed peptide folds.

Combining a fixed orientation with a structured but tunable environment will expand the range of uses for small molecule/peptide adducts and allows for simpler, more precise modeling studies to be carried out. Potential applications are not limited to biotechnology; the small molecule could also be chosen for its catalytic activity. Structured peptides could provide a secondary coordination sphere for catalyst substrates [10,30–32], mimicking enzymatic sites. In the case of the peptides used herein, very few residues (nine) are required to achieve a designed, fully folded structure.

The Beta Cap Peptide, or Captide

We have already demonstrated a modular β -cap motif that provides significant (>6 kJ/mol) stabilization at the terminal ends

of any antiparallel beta sheet (e.g., the termini of a hairpin peptide), [33,34] due in large part to the interactions of cross-strand tryptophan residues [35,36]. Curiously, we found that this β -cap motif absolutely required an *N*-amide unit for folding; acetyl and propanoyl ($\text{CH}_3\text{CH}_2\text{CO}-$) were used in the prior studies. We initially reported [34] alkanoyl-WlpGXTGPS-NH₂ ($\mathbf{p}=\text{D-Pro}$, $\mathbf{X}=\text{Leu}$ or Ile) species that were $\geq 97.5\%$ folded at 280 K in water ($\chi_F \geq 0.975$). We have since established that a diverse array of small molecules can replace these alkanoyl units. Here, we show that small molecules (R) were attached *N*-terminally to a slightly less stable β -cap motif ($\text{RCO-WlpKKWTGP-NH}_2$) adopt specific, rigid conformations relative to the capped hairpin. We show that the same rules apply on extension to larger, capped β -sheet structures (e.g., RCO-WTVTIGHKKIRVVTGP-NH₂). We have given these capped β -structures the general name 'captides': any beta sheet terminating in a rigid joint with nearly any small molecule carboxylic acid derivative. When the small molecule is a di-carboxylic acid, it forms a joint or hub between two β -sheets set at specific angles.

The choice of an IpKK turn rather than the original IpG-(L/I) unit served two functions: (i) it reduced fold-fraction to the point ($\chi_F=0.92-0.94$ for $\text{R}=\text{CH}_3-$ and CH_3CH_2-) where superior small molecule candidates could be identified by monitoring NMR shifts, and it provided solubilizing Lys sidechains to offset the effects of larger apolar *N*-terminating groups. In the absence of an *RCO* group, the peptide displayed no measurable formation of a hairpin-like structure.

* Correspondence to: Brandon L. Kier, University of Washington - Chemistry, Bagley Hall Room 205 Box 351700, Seattle, Washington 98195-1700, USA. E-mail: sciguy@u.washington.edu

University of Washington - Chemistry, Bagley Hall Room 205 Box 351700, Seattle, WA 98195-1700, USA

Essential Features of the Beta Cap

The sequence of this peptide, and β -capped peptides in general, includes a mix of essential and mutable residues. We have previously discovered [33] that the loop region can be swapped for a longer beta hairpin or open-ended sheet, and the C-terminus can be extended indiscriminately, but the beta-capping residues must be conserved. We determined that, for our minimalist system, W1 is essential and T7, I2, D-Pro3, and G8 are strongly preferred. K4 and K5 could be any residue, P9 could be any residue or simply deleted, and W6 could be any aromatic residue. We re-confirmed these residue requirements in the context of larger RCO- N-terminating units, with W6Y, des-P9, and K4H and K5H mutants; see Supporting Information, Sections S3 and S5 for details.

The minimalist motif used herein corresponds to $n=0$ in the structural depiction in Figure 1(A). A longer beta-capped hairpin ($n=2$) with an IHGK turn was used to verify that small molecule caps were viable for longer hairpins (shown in Figure 17 and discussed further in Section ‘Captides from longer β -capped peptide structures’ in the results).

Fold-fraction quantification via chemical shift deviations (CSDs)

Observed chemical shifts, recorded as CSDs from statistical coil norms, are population-weighted averages. Thus, χ_F (the fraction folded) can be equated with $CSD^{\text{obs}}/CSD^{100\%}$; the 100% values were calculated previously via amide H/D exchange [34] and confirmed by comparison with values from the best-folded

captides of this study (see Supporting Tables S2–S4 for raw chemical shift data). Because small stable peptides have broad thermal melting transitions, measurable unfolded populations (typically 2–12%) persist at temperatures well below the T_m , which is typically 60–80 °C for most constructs of the form RCO-WlpKKWTGP-NH₂. Characterization at a single temperature well below the T_m (typically 280 K in the present study) can provide relative stabilities; the same is not true of proteins with sharp thermal transitions.

Spectroscopic diagnostics of the beta cap

β -capped peptides are easily characterized by NMR and circular dichroism. The edge-to-face indole/indole geometry produces a very large CD exciton couplet (with a $\lambda=228$ nm maximum) and upfield shifts in the facing aryl-H sites of the edge indole, typically a 2.4 ppm upfield shift at W6-H_{e3} for a fully folded species. The Gly amide to indole ring H-bond illustrated in Figure 1(B) results in an even larger upfield shift (>3 ppm at 100% folded CSDs) for this amide proton. These are examples of characteristic CSDs. Other large CSDs that report on β -hairpin and turn formation are seen at K4H_n, K5H_a, and I2-H_n; these sites have theoretical 100% folded CSDs of 0.5, 0.54, and ~1.5 ppm (see Section S15 in the Supporting Information). We anticipated that these CSDs would be minimally affected by subtle alterations to the cap caused by different small molecule attachments and would thus reliably report on overall fold populations of our constructs: this proved to be the case.

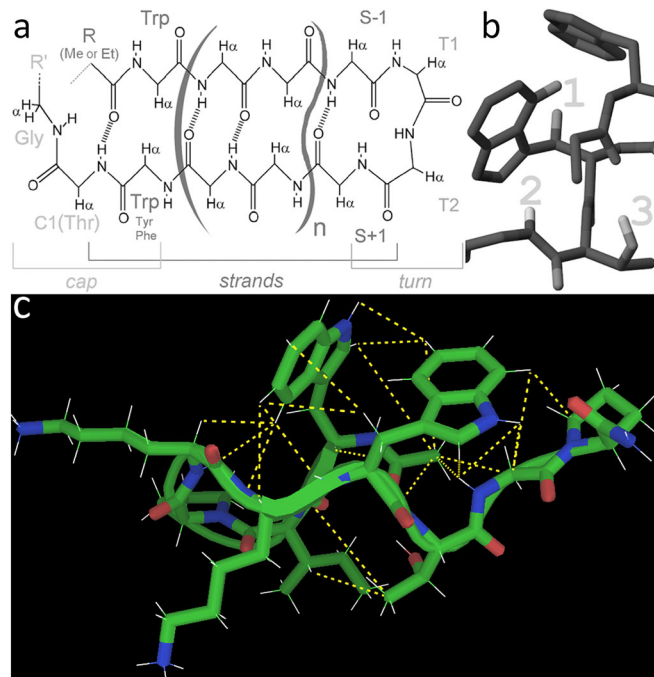
Materials and Methods

Materials

All small molecule carboxylic acids were purchased from Sigma-Aldrich except for the methyl cymantrene carboxylic acids, which were synthesized via a variant of Friedel-Crafts acylation [37,38]. Dimethylsuccinic acid, 1,2-dicarboxylic acid cyclopentane and 1,4- & 1,3-dicarboxylic acid cyclohexane were purchased as racemic mixtures; the resulting isomeric captides had very different structural properties and were easily separated via HPLC.

Peptide synthesis

Peptides were ordered from GenScript as resin-bound protected chains or synthesized manually. Manual synthesis, and N-terminal small molecule attachment, was accomplished via standard amide ligation techniques with HATU/HOAt or COMU as coupling agent, DIEA base, NMP (*N*-methyl pyrrolidone) solvent; coupling steps alternated with Fmoc deprotection steps (20% piperidine in NMP) for the synthesis of complete peptides. Our only deviation from a standard amide bond formation procedure (Fmoc chemistry) was our reduced ratio of small molecule to peptide, when attaching two or more peptide chains to a polycarboxylic acid. In this case, a 1.5 : 2 or 1.5 : 3 ratio of small molecule to on-resin peptide was employed, rather than the 4 : 1 ratio standard to peptide synthesis. Tetrameric acids were triple-coupled to on-resin peptide with a near-stoichiometric (approx. 1 : 5 peptide amine per tetra-acid, or 1 amine per 1.25 carboxylic acid group) ratio of polyacid to free amine per coupling for final yields in excess of 50%. Cleavage from resin and sidechain deprotection was carried out in 95 : 2.5 : 2.5 trifluoroacetic acid (TFA)/triisopropylsilane (TIPS)/H₂O. Cleavage times were 1–2 h for adducts of monoacids and 2–4 h for adducts of polyacids. All captides were purified in-house via RP-HPLC



using C₁₈ and/or C₈ stationary phases and a water (0.1% TFA)/acetonitrile(0.085% TFA) gradient. HPLC peaks for unligated and/or partially ligated peptides were frequently observed as major byproducts; partially ligated peptides dominated if the reaction mixture was too rich in the polycarboxylic acid, whereas unligated peptides dominated if the ratio was perfectly stoichiometric or lighter on the polycarboxylic acid. Identities were confirmed, and yields qualitatively assessed, by the molecular ions observed on a Bruker Esquire ion-trap mass spectrometer (Bruker Daltonics).

Characterization: CD

CD samples at 30 μM were prepared in aqueous pH 7 20 mM potassium phosphate buffer; concentrations were determined using the molar absorptivities of Trp and Tyr, as well as those of aromatic small molecules (determined as the free acid at the lowest possible pH for analogy to their peptide-bound amide forms). Spectra were recorded on a Jasco J720 spectropolarimeter (Jasco Inc.) using 0.10-cm pathlength cells over a default range of 190–270 nm. Thermal melts were plotted as the change in temperature *versus* the absorptivity of the positive 228 nm peak (Trp/Trp exciton couplet maxima). CD data (both raw data and thermal melts) for selected captides appear in the Supporting Information, Section S13.

Characterization: NMR

Samples for 2D NMR spectral studies consisted of ~1 mM peptide in 50-mM phosphate buffer (typically pH 7), 10% D₂O, and 4,4-Dimethyl-4-Silapentane-1-Sulfonic acid as an internal chemical shift reference. NMR experiments were collected at 500 or 700 MHz on Bruker DRX and AV spectrometers (Bruker Biosciences Corp.). Full ¹H spectral assignments were made by using a combination of 2D NOESY and TOCSY experiments. Typical NOESY mixing times were 175 ms. Complete assignment of all non-exchanging protons could be made for all peptides, excepting certain rare cases of extreme line broadening (peak disappearance). The H_N and H_α CSDs were calculated using the CSD_b algorithm [36,39]. Fold populations were derived from CSDs as previously described [33,34,36,39–42]. Further details concerning the derivation of fold populations and standard deviations appear in the Supporting Information, Section S14.

Results and Discussion

We examined over 50 different captides, each containing the same capped-beta peptide but a diverse assortment of monocarboxylate or polycarboxylate small molecules at the *N*-terminus. Attachment of the capping molecule was a simple matter of extending peptide synthesis by one coupling reaction. The polycarboxylic acids (amides, on ligation) with multiple attached peptide moieties are viewed as ‘hubs’. The small molecule acids were selected for diversity (aryl/alkene/alkyl, large/small, hydrophobic/hydrophilic, mono/di/tri-acids, etc.) to provide a complete-as-possible test of the strengths and limitations of the captide system. We also took functionality into account: we investigated captides incorporating molecules that are strongly metal-ligating, reversibly redox-active, have a high neutron cross-section, and common fragments used in medicinal chemistry.

Spectroscopic diagnostics of the resulting captides

As expected, the captides displayed the CD exciton couplet and ring current shifts due to the indole–indole interaction, as well as all expected NMR diagnostic shifts (far-upfield G8-H_N and the

backbone H_N and H_α CSD indicators of hairpin formation). The latter was used to estimate 280 K fold- fraction; the results are compiled in Figure 2.

Whereas the chemical shift patterns (and thus structure) of the beta cap remained remarkably consistent, some adduct-dependent variations were observed, most notably in the CSD ratio between H_{ε3} and H_{δ1} protons of Trp6, which report specifically on the χ_2 rotamer (predominantly +80° for R=Me or Et). For certain larger groups, we observe varying proportions of the $\chi_2 = -100^\circ$ conformer, where the H_{δ1} (as opposed to H_{ε3}) proton of Trp6 points toward the indole ring of Trp1 – likely to alleviate a steric clash between Trp6 and the bulky adducts (see section S2 of the Supporting Information for more information).

Finally, the amide proton of Trp1 also provided information regarding the interactions between the small molecule and folded peptide. As the first proton of the peptide chain, its NOEs and CSDs can vary drastically depending on what is attached at the *N*-terminus. W1 H_N NOEs report on local conformation and when the *N*-terminal small molecule is aromatic (e.g., the residue of a benzoic acid analog), W1 H_N CSDs can be used to gauge approximately how close the ring and amide bond are to planarity. We observed downfield ring current shifts as large as 4 ppm at this amide H_N (see Supporting Information, Section S8 for more information).

General stability trends: which small molecules work best/not at all

There are a number of trends and lessons that arise from the characterization of captides with a broad set of small carboxylic acid residues at the *N*-terminus. Foremost, among these lessons: an impressively diverse array of carboxylic acids produce well-folded captides. This is perhaps surprising, given that these molecules are invariably at least half-buried by the peptide moiety upon conjugation. Furthermore, the captide structure remains remarkably consistent across almost all adducts; the only alternate structured conformers are a variant with a reversed Trp6 χ_1 angle (see Supporting information, Section S2) and a variant with an alternative Gly8 orientation (see Supporting Information, Section S4).

Even the exceptions, carboxylic acids that result in only partly folded adducts, still display peptide fold populations that are significantly larger than the peptide with a free amino terminus. These peptide folding failures are typically the combined result of steric bulk and improper shape (e.g., xanthene 9-carboxylic acid inhibits folding of the captide due to steric clashes with the folded state) or stoichiometry (e.g., trimesic acid yields well-folded adducts when attached to one or two chains, but three chains cause fold inhibition due to interchain clashing). Indeed, *diastereomers* of many of these fold-inhibiting adducts have well-defined structures that are fully formed. For example, in contrast to their poorly folded R-isomers, the captides of S 2-phenylpropanoic acid and S,S' dimethylsuccinic acid are nearly 100% folded at 280 K.

Structural implications of adding small molecules to the beta cap

We have established that the orientation of the small molecule relative to the peptide, and the conformations that result, follows a set of defined rules. All but the simplest molecules (e.g., acetic acid propionic acid) have rotatable bonds – and these bond angles are observed to remain fixed in one or two populations, depending on the molecule. These features are presented for each class of carboxyl groups below. Refer to Figure 2 or Section 16 of the Supporting Information for the complete list of all 70+ captides.

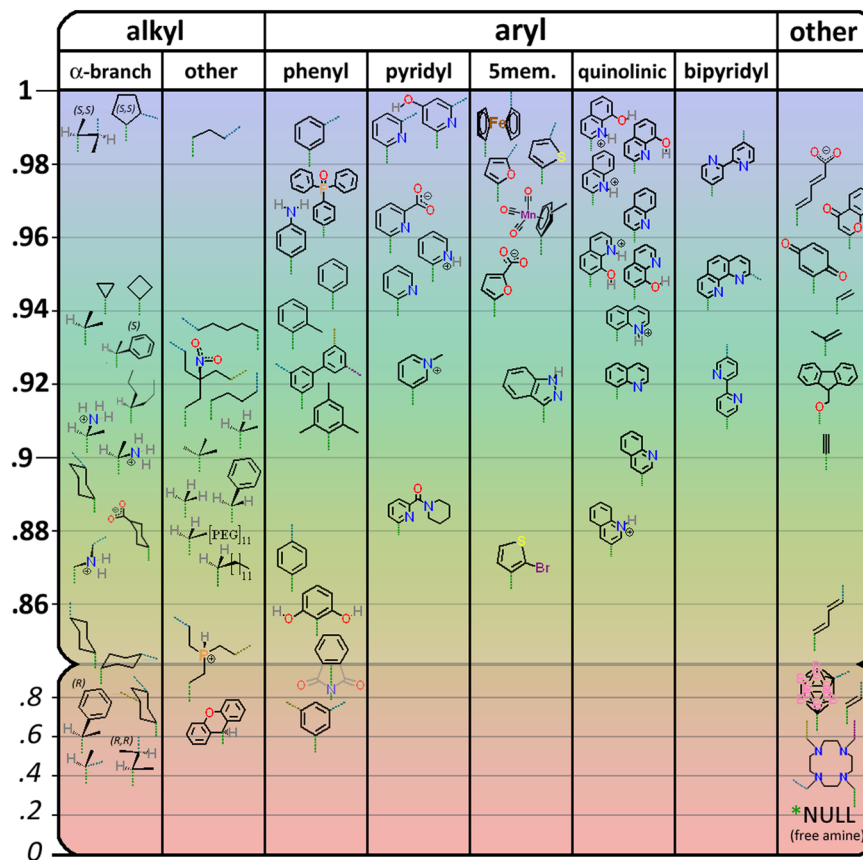


Figure 2. Fold populations at 280 K for RCO-WlpKKWTGP-NH₂ display a dependence on the nature of R. The downward-pointing green dotted line represents the position of the carboxamide linkage between the small molecule R group and the peptide. 'α-branched' represents the subclass of alkyl carboxylic acids with two R groups (methyl for the parent compound: isobutyric acid) and one hydrogen alpha to the carboxyl. Cyan, dark yellow, and magenta dotted lines represent second, third, and fourth symmetric attachment points for polyfunctional acids (see Supporting Information, S15 for the complete table of CSDs and ΔG_fs and less crowded versions of this figure containing only monoacids or only polyacids.)

Peptide Adducts of Monocarboxylic Acids

Alkanoyl capping groups

Of these, alpha-branched acids (e.g., isobutyric acid) form the most stable and rigidly oriented adducts (see Figure 3). There is a preference for two of the alpha-substituents to be small – optimally, one hydrogen and one small alkyl group (e.g., methyl) in the pro-R position. A single hydrogen substituent at the alpha position aligns with, and in the plane of, the amide proton (as evidenced by a very large NOE). The pro-R alkyl group is observed to pack tightly against both indole rings (sequestered from solvent), and the pro-S group is oriented outward, exposed to solvent. It is this pro-S position that is amenable to substitution by almost any other group, whereas there is a size limit at pro-R. For example, S phenylpropionic acid (isobutyric acid with the pro-S methyl replaced by phenyl) possessed roughly identical stability and structure *versus* its highly structured parent, the isobutyric (α-dimethyl) adduct. R phenylpropionic acid, however, was significantly less stable (~70% folded at 280 K, ΔΔG > ~3.8 kJ/mol). Additional examples of alkyl substituent effects appear in the Supporting Material (Section S6).

Aryl groups

Aromatic carboxylic acids follow a more complex set of conformational rules; even the simplest case, a benzoyl group, adopts two near-equivalent conformers. Benzamide bond conjugation competes with steric repulsion between amide and

ortho-phenyl protons, such that the lowest energy conformations are plus and minus approximately 26° between the amide and benzene planes [43–45]. See Figure 4.

This angle cannot be calculated precisely by NMR although we possess good qualitative indicators: the amplitude of the NOE between amide and the *ortho* proton(s) and enhanced CSDs from statistical coil norms; large positive chemical shifts indicate more nearly planar orientations. When the aryl–amide rotamer is within ~30° of planarity, one face of the aryl ring packs against the Trp 6 indole, whereas the other remains solvent exposed. This results in large ring current shifts and in combination with the intermediate speed of rotation of the benzamide bond rotation, significant broadening of the NMR peaks of the amide 1 proton, the six-membered ring protons of Trp 6, and the *ortho* and *meta* protons of the benzoyl ring. This broadening is only observed when the positive and negative benzamide rotamers have near-equivalent energies, as is the case for symmetric species (e.g., the adduct of benzoic acid; Figure 5).

Aryl groups substituents at *ortho*, *meta*, and *para* positions have different effects on packing interactions.

Ortho substituent effects. Ortho substituent(s) can tune the ring-plane to amide-plane angle and thus the orientation of the aromatic small molecule adduct relative to the peptide chain. Hydrophobic *ortho* groups force benzamide bond angles higher [44,45]. For example, 2,4,6-trimethylbenzoic acid is oriented nearly antiplanar. As part of a captide, its two *ortho* (2,6) methyl

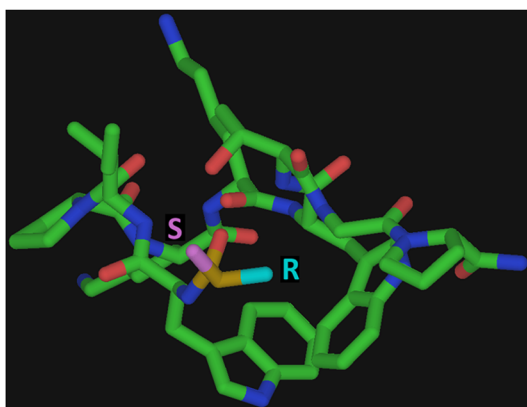


Figure 3. Top: the very different environments of the Pro-S (solvent exposed) and Pro-R (buried) groups of alpha-branched substituents (isobutyric acid in this case). This geometry is maintained by the propensity of the alpha hydrogen to align (offset by approx. 20°) with the amide proton. However, this is not the case when one methyl group is changed to the isosteric NH_3^+ (as per L or D Ala) in which the case charged amine packs itself against the tryptophan (buried position, NOT solvent exposed), and for both cases, the overall fold of the captide is altered slightly (see Supporting Information, Sections S2 and S4 for more details). Bottom: The general form of the ideal captide *N*-alkyl group. To our knowledge, X and Y can be any groups. The $\Delta\Delta G$ for replacing a small Pro-R alkyl group with a hydrogen (e.g., for isobutyric vs propanoic acid) is less than 1 kJ/mol; alpha branching is technically ideal but by no means essential.

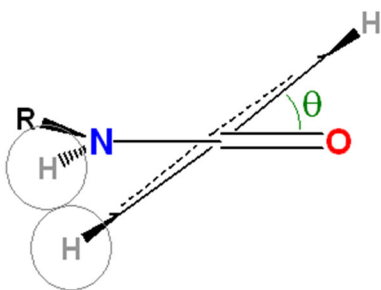


Figure 4. The angle between benzene ring and amide bond is ~26° by default but can vary (generally increasing) depending on the presence of modifications at one or both *ortho* positions.

groups slowly swap, via hindered benzamide rotation, between buried and exposed environments. This intermediate-timescale exchange results in extremely broad NMR signals relative to the *para* (4) methyl group.

Polar groups and pyridyl nitrogen non-bonded electron pairs can have the opposite effect. They provide a 'hole' and/or H-bond acceptor for the amide proton or a donor for the carbonyl oxygen. This biases the benzamide bond angle toward planarity, as conjugation and H-bonding effects can outweigh steric concerns. However, larger *ortho* groups (e.g., oxo-diphenylphosphine) disallow folding altogether because of extreme steric clashing with

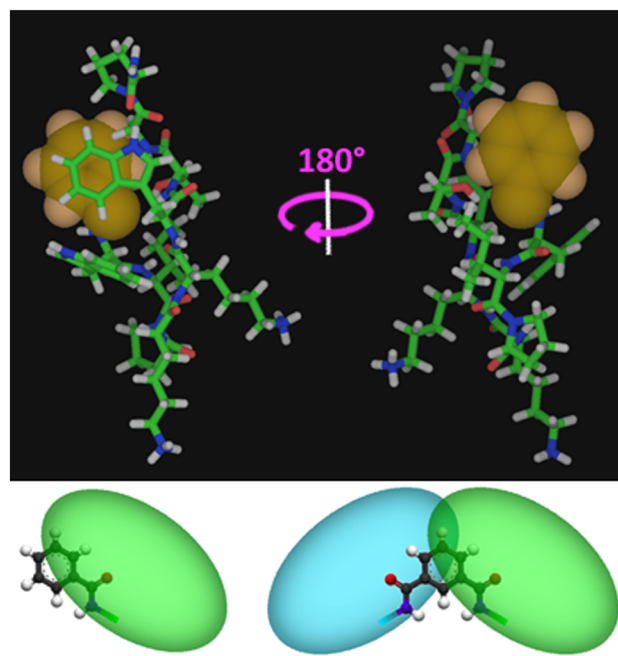


Figure 5. The 'captide', with the *N*-terminal unit highlighted. 'Top' and 'bottom' views (180° rotation) illustrating the nature of packing against aromatic *N*-terminal attachments for this peptide. One face of the ring is entirely covered, whereas the other is entirely exposed. Two peptides attached to the same ring results in a fully buried ring. Bottom: cartoon representations of how attached peptide chains pack against benzoic and isophthalic acid.

Trp6 in the folded state (more detail on *ortho* substituents, benzamide bond rotation, and very positive CSDs in the Supporting Information, Section S8. For more detail on aromatic substituents in general, see Section S7).

Meta and *para* substituent effects. *Para* positions of an attached benzamide moiety are amenable to diverse substitution. Captide folding propensity greater than or equivalent (within error) to that of the benzoic acid parent was observed for both large and small *para* substituents (see Figure 2). Bulky groups (e.g., oxo-diphenylphosphine) increased peptide fold-stability likely because of packing interactions with the Trp rings. However, these groups also slow benzamide bond rotation and further broaden NMR resonances, such that specific NOEs are difficult to discern (further discussion in the Supporting Information, Section S2).

Meta positions are similarly permissive of diverse substitution. In the context of the beta-capped peptide, they also become non-equivalent: the *meta* position nearest the benzamide carbonyl is partly buried, whereas the *meta* position nearest the benzamide proton is almost fully exposed. Many asymmetrically *meta*-substituted rings showed little selectivity between these two positions, as evidenced by nearly equal intensity NOEs between the benzamide proton and the two distinct *ortho* protons. However, charges on the ring can introduce a conformational preference. Upon protonation of the quinoline 3-carboxylic acid adduct, the NOE ratios suggest a shift from a mixed population to a single rotamer: a rotamer, which allows solvent access for the NH^+ (see Figure 6).

Alkenoyl groups

Adducts of alkenoic acids behaved similar to their aryl and alkyl counterparts, but with one interesting distinction. Stronger

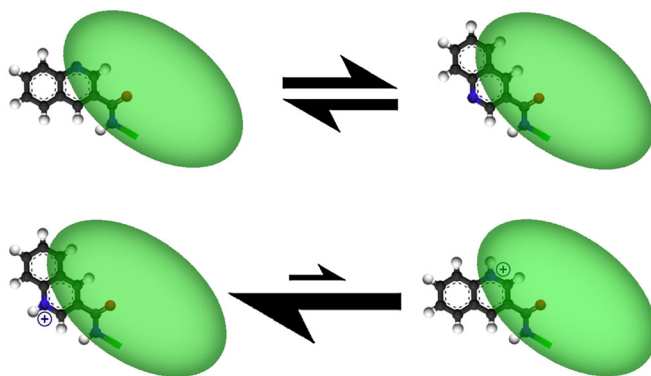


Figure 6. Quinoline 3-carboxylic acid illustrates how protonation state (and thus pH) can influence the conformation of small molecule bound captides: the green region is a cartoon representation of the peptide chain. Rotamer populations were determined via NOE intensities between amide and *ortho* protons. More details appear in the Supporting Information, Section S11.

conjugation between alkene and amide bonds led to *cis/trans* isomerism, readily distinguishable as separate sets of sharp peaks not only by NMR but also by HPLC (see Figure 7). This conjugation/slow exchange effect was also observed for the adducts of weakly aromatic furan 2,5-dicarboxylic acid and 2,5-dihydroxybenzoic acid (which likely exists as the (partially) oxidized (hydro)quinone).

Other monofunctional carboxyl units

A range of other more unusual adducts was investigated; in all cases, the only limiting factor for captide fold-stability was the steric bulk of the carboxylic acid. For example, long PEG11 carboxylic acid (*O*-(methyl)-*O'*(2-carboxyethyl)-undecaethyleneglycol) folded in a manner equivalent to the analogous propanoyl captide (fold population of 87% vs 90% for propanoyl), whereas bulky *m*-carborane C,C-diacid and xanthene 9-acid were significantly less stable. Fmoc, with its thin spacer followed by a bulky capping unit, made close contacts with both Trp rings and was not fold-destabilizing.

Polycarboxylic acid hubs yield peptide 'dimers'

Small molecule attachment to beta-capped peptides is not limited to monocarboxylic acids. Amide ligation can be repeated

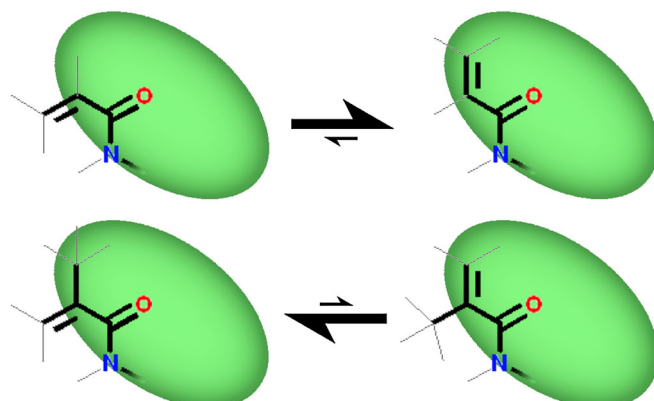


Figure 7. Alkene-conjugated amides are fixed in one of the two planar conformers, interconverting on the seconds to hours timescale. Acrylic and Methacrylic captides had opposite E/Z preferences: NMR peak intensity ratios suggested that the dominant species was >90% populated in both cases. The interconversion of the methacrylic acid adduct was slow enough to provide conformers that could be resolved via HPLC.

multiple times, producing dimeric and even trimeric or tetrameric peptides centered at a small molecule hub. The orientation and rigidity relating the peptide chains is determined by the small molecule hub and varies considerably between aryl, alkyl, and other attachments.

In the subsequent figures depicting captide dimer structures, only obligate interchain NOEs (NOEs that are impossible for a structured captide monomer) are shown. We found that the intrachain peptide conformations, as indicated by the expected NOEs and CSDs, were effectively identical in all cases. Even in cases where the carboxylic acid hubs oriented the peptide chains such that some steric clashes resulted, the folded-state conformations of peptide segments were preserved. The only significant change for poorly oriented dimers was decreased folded-state population, a result of the incompatibility of two simultaneous fully structured peptide chains.

We did not fully elucidate NMR structures for each example but constructed and confirmed our models via analysis of obligate interchain NOEs (justifications of our assignments of inter vs intrachain NOEs appear in the Supporting Information, Section S9).

Dimeric adducts of alkanoic acids

Because alpha-branched acids (analogs of isobutyric acid) proved optimal for forming stable monomeric captides, we investigated alpha-branched di-acids as saturated dimerizing hubs. The previously observed stereochemical requirements are reaffirmed here. Small (e.g., methyl) and large (e.g., phenyl) substituents are allowed at the respective Pro-S and Pro-R positions, respectively. The large (optimally Pro-S) substituent in this case is the second identical peptide chain.

HPLC purification of the ligation product of the WlpKKWTGP-NH₂ peptide and dimethylsuccinic acid afforded three readily separated peaks, corresponding to the SS, RS, and R,R diastereomers. The R,R diastereomer was shown by NMR to be poorly folded, whereas the R,S diastereomer showed distinctly different fold populations for the two isomeric chains. The S chain adopted a standard hairpin (captide) fold, whereas the R chain was largely unstructured (though its modest residual structure was still predominantly that of the expected captide hairpin). The S,S diastereomer produced a fully structured homodimer, with record-breaking chemical shifts at the Gly 8 H_N (shift = 4.08 ppm; CSD = -4.136 ppm). The compact interchain interface could be elucidated via numerous obligate interchain NOEs, see Figure 8.

The analogous dimer with a S,S (trans) 1,2-dicarboxylic acid cyclopentane hub was also investigated, see Figure 9. Modeling suggested this to be the optimal saturated captide dimer; similar to the S,S dimethylsuccinic hub but with an entropy bonus to stability due to the lack of rotatable bonds within the hub. It proved to have slightly higher fold stability and, as expected, a similar interchain interface.

We also investigated the captide adducts of increasingly long alkane di-acids. Glutaric acid (two carboxylates separated by three methylenes) was a surprisingly fold-stabilizing hub, with a captide fold population approaching unity (see Supporting Information, Figure S1c for a potential structure). Longer adipic and pimelic di-acids (four and five methylenes, respectively) displayed no special fold enhancement. Adipic and pimelic di-acids were roughly equivalent to their single chain propanoic acid analog (adipic was slightly worse, at 85% captide structure formation, vs 90% for both pimelic and propionic). Alkyl dimers with fold populations below that of their single chain propionic

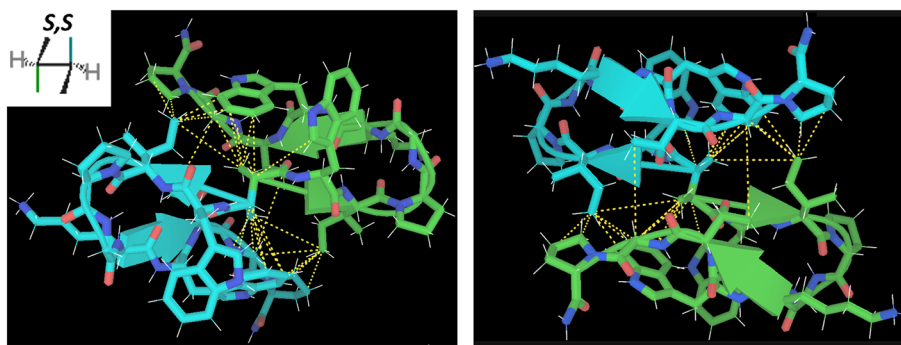


Figure 8. Two different views of an optimal alkyl captide covalent dimer about S,S-dimethylsuccinic acid. The structure was validated by numerous interchain NOEs (dashed yellow lines). Many of these NOEs involved the Ile 2 sidechain; in fact, this was true for most two-chain captides. We consider Ile2 to be generally important for interchain (but not intrachain) peptide packing.

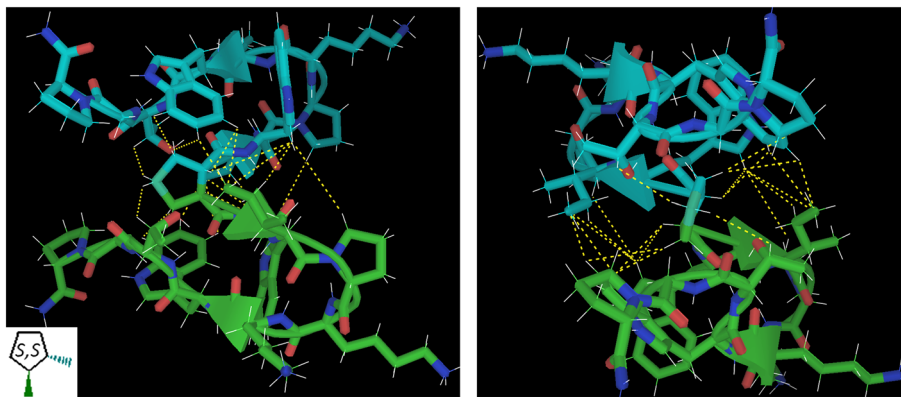


Figure 9. Similar views of 1,2-S,S-dicarboxylic acid cyclopentane. The NOE-confirmed models of S,S-dimethylsuccinic acid (Figure 8) suggested 1,2-S,S-dicarboxylic acid cyclopentane as an optimal small molecule hub for dimerization. The packing of the cyclopentane hub against four Trp rings resembles other optimized aryl/pro interactions common to hyperstable miniproteins, such as the Trp-cage and WW domain. $\Delta\Delta G$ between this folded state and the unbound monomer is in excess of 10 kJ/mol per chain even at room temperature.

or isobutyric controls included the adducts of *cis* and *trans* 1,4 dicarboxylic cyclohexane and methylmalonic acid (detailed fold population data appears in the Supporting Information, Section S15).

Dimers about aromatic hubs

Aromatic rings were expected to be ideal dimerization hubs. Peptide chains were observed to bury exactly one face of a phenyl ring, thus leaving the other face free to pack against a second peptide chain. We sought to confirm this hypothesis and determine which position (*ortho*, *meta*, or *para*) was ideal for interchain packing.

The dimer of terephthalic acid displayed very poor line shapes and two sets of peaks in NMR. This was not surprising: *para* positioning of two peptide chains results in two redundant symmetry axes and thus multiple semi-equivalent options for interchain orientation. The existence of two sets of broadened peaks suggests moderately slow interconversion between the two possible symmetry forms; see Figure 10. The dimeric *ortho* form (starting from phthalic acid) could not be synthesized using standard amide coupling methods; the structured but single chain phthalimide form was observed instead. The *meta* orientation, e.g., isophthalic acid hub, proved ideal. In this orientation, the two-folded peptide chains have minimal contacts; very few obligate interchain NOEs were observed.

Heteroatomic aromatic hubs

Heteroatom-containing analogs of isophthalic acid adopted nearly identical structures, with CSDs suggesting even higher fold

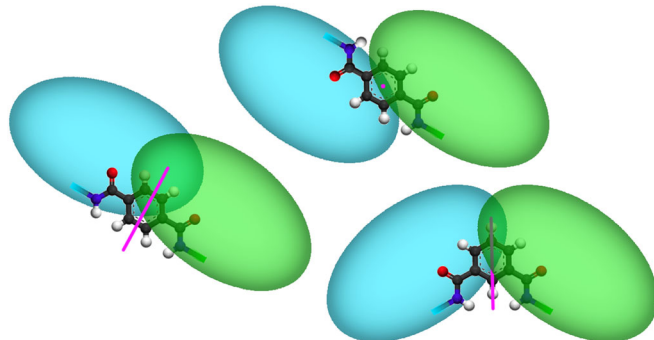


Figure 10. Left and top: The two symmetric forms (*cis/trans* or *Z/E*) of the terephthalic acid captide adduct, with C₂ symmetry axes in pink. Two sets of broad peaks are observed by NMR indicating that these conformers exist in equilibrium, interconverting on a rather slow timescale. Bottom right: the isophthalic acid dimer, which contains only one symmetry axis. This construct had a very high fold stability ($\chi_F > 0.95$) and displayed a single set of sharp resonances.

populations (~95–99%). The reason for the slight fold improvement of the captides of dipicolinic acid, thiophene 2,5-diacid, and furan 2,5-diacid *versus* isophthalic acid was likely the missing inner-*ortho* proton. A centrally located 'inner *ortho*' heteroatom leaves a 'hole' for the two amide proton 'pegs' to fit into. See Figure 11 for the structure of this captide dimer fold family.

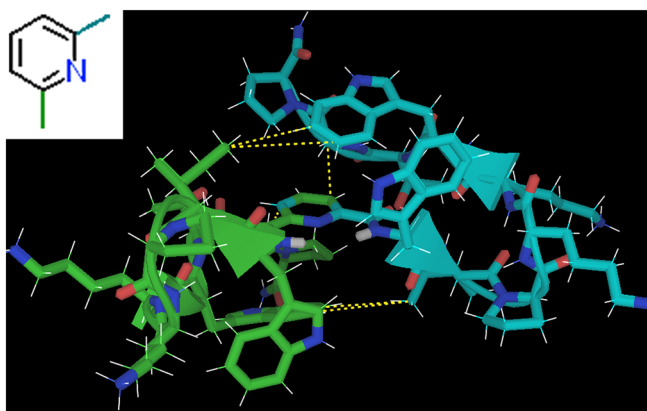


Figure 11. The captide dimer di-adduct of picolinic acid, an optimal single-ring aromatic-hub. The structure was validated by interchain NOEs. These are highlighted in yellow; note that there are significantly fewer than for the dimethylsuccinic hub. The peptide chains are held at specific angles despite an almost total lack of interfacial packing; the central hub is fully buried. The isophthalic acid dimer displayed essentially the same interchain NOEs, although the technically non-planar benzamide angles resulted in slightly different interchain packing. The isophthalic acid form also exhibited a very large NOE between W1 HN and the inside *ortho* proton, establishing the rotameric state of the benzamide bond.

Multi-ring hubs

Of the two-ring hubs we investigated, all displayed fold populations equivalent to (within error) or above those of the monomeric parent: the benzoic acid captide. This is in contrast with the single-ring hubs, which resulted in two-chain captides better or worse folded than their parent, depending on the relative positions of the carboxamides. Multi-ring hubs should have fewer possibilities for interchain clashing *versus* single-ring hubs, due to the rotatable bond between the rings and/or the greater distance between chains.

The 1,1'-dicarboxylic acid of ferrocene proved to be the most fold-stable captide dimer; interchain NOEs indicated that it adopts a z-displaced isophthalic type structure (the z-axis in this case being the line intersecting the cyclopentadienyl centroids and iron), see Figure 12.

The other two-ring systems we investigated were 2,2'-bipyridine dicarboxylic acids (4,4'-acid and 5,5'-acid; see Figure 13 for the former) and phenanthroline 2,9-dicarboxylic acid. All three exhibited high fold stability.

Beyond dimers

Trimmers, with three peptide chains attached to a central ring, proved to be poorly folded. Simple models suggested that there was no room for a third peptide chain; each chain covers precisely one face of a ring. Hairpin fold populations were observed to be ~65% for both the tri-adducts cyclohexane *cis*, *cis* tricarboxylic acid, and 1,3,5-benzene tricarboxylic acid: only two of three peptide chains can adopt the folded conformation. For comparison, cyclohexane *cis* 1,3-carboxylic acid and isophthalic acid yielded dimeric captides with fold populations of 92% and 96%, respectively. (A 1,4 arrangement of two chains about either cyclohexane or benzene rings results in lowered captide fold populations nearer to those of the 1,3,5-arranged three-chain captides. Direct comparisons between two and three-chain captides require that the hubs have equivalent geometries).

It appears that one consequence of the one-face/one-peptide packing about aroyl hubs is a two-peptide limit per ring. Thus,

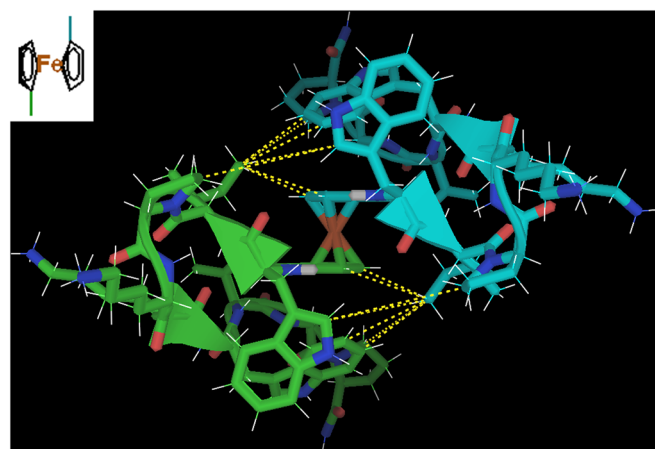


Figure 12. An NMR-justified mockup structure of the ferrocene-peptide dimer. These justifying interchain NOEs are highlighted in yellow; the Ile2 H81 methyl has a very large number of NOEs and a significant downfield shift (unsurprising, given that this methyl group is in-plane with multiple aromatic rings). The peptide chains are held at specific angles despite the free rotation of the cyclopentadienyl rings about the central iron.

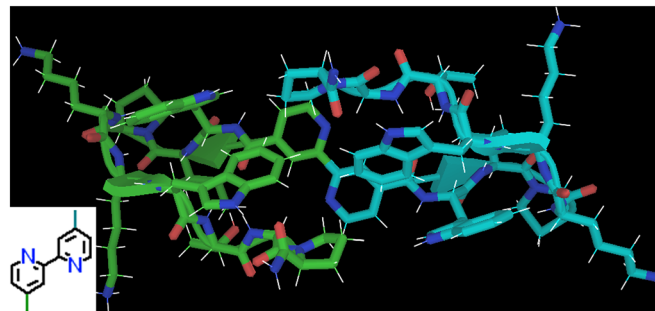


Figure 13. The captide of 2,2'-bipyridine 4,4'-dicarboxylic acid. No specific structure could satisfy all observed NOEs, suggesting the possibility of a second dimerization affording a D2-symmetric species. This additional 'dimerization' does not represent hexamerization around Bpy, which was incomplete even in the presence of Fe II ions, and would also have resulted in a dramatic color change, which was not observed.

we expected that higher-order constructs would prove viable so long as the small polyacid hub contained multiple rings. We were able to synthesize 1,3,5-Tris(4-carboxyphenyl)benzene (W1pKKWTGP-NH2)₃, but line shapes were too poor for characterization – either because of oligomer formation via the hydrophobic hub or (more likely) the six different medium-slow rotating aryl–aryl and aryl–amide bonds resulting in dozens of near-equivalent conformers.

We finally achieved a well-folded three-chain captide by using flexible, C3-symmetric tri-acids as hubs: nitromethane trispropionic acid and tris(carboxyethyl)phosphine. The former produced a three-chain captide with a χ_F of 0.91 (fold population of 91%). For comparison, the two-chain pimelic acid hub has the same number and type of rotatable bonds between chains, and the single chain propanoic acid captide can be considered a 'one-armed' fragment; all three of these captides (one, two, and three chains) have roughly the same fold populations. This suggests that the three folded peptide arms neither clash with nor pack efficiently on their symmetric partners. NOEs and modeling can rule out many potential interchain packing geometries but cannot establish the supremacy of any specific

orientation; this three-chain captide likely exists as an ensemble of related conformers (see Supporting Information, Section S1 for more details and one potential structure).

Regarding tetramers, we had some success with the four chain captide adduct of $(WlPHHWTP-NH_2)_4$ Biphenyl-3,3',5,5'-tetra-carboxylic acid. This construct's chemical shifts (NMR) and exciton couplet (CD) were characteristics of a near-fully folded captide. Yields were reasonably high (~50%) despite the necessity of four separate resin-bound peptide amide ligations to each hub molecule, see Figure 14.

The tetrameric peptide adduct of 1,4,7,10-Tetraazacyclododecane-1,4,7,10-tetraacetic acid was also successfully synthesized at reasonable yield using straightforward on-resin strategies, but it proved to be very poorly folded and gave broadened uninterpretable NMR spectra.

Proof-of-concept Applications and Implications

Methyl cymantrene and catalysis

The ferrocene captide dimer is a remarkably stable metal-peptide framework, both in folding ($T_m > 85^\circ\text{C}$, 280 K, $\chi_F = 0.98$) and chemical terms. We have established that only one face of the ring is buried per peptide chain, thus it seemed reasonable to assume that we could effectively cut the ferrocene dimer in half and access the reactivity of the metal site. Many transition metals can form highly stable mixed cyclopentadienyl/carbon monoxide compounds. The classic example is cyclopentadienyl manganese tricarbonyl (also known as cymantrene), with chemical stability approaching that of ferrocene, yet containing smaller, more labile monodentate ligands in place of the second Cp ring. Although cymantrene itself is inert unless its CO ligands can be exchanged, it is part of a structural class that includes a wide range of catalytic compounds [46]. Furthermore, peptide adducts of cymantrene and the analogous technetium compound have been the subject of considerable study [47–50], due in part to the technetium's usefulness as a bio-radiotracer. This prompted us to examine captides based on this type of hub (Figures 15 and 16).

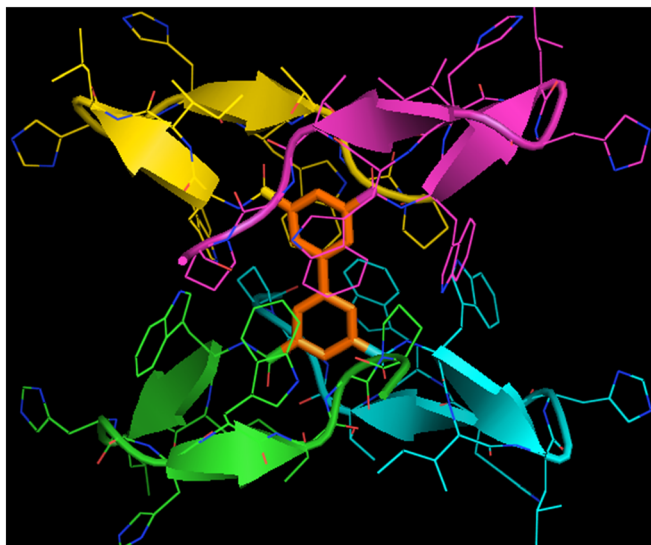


Figure 14. Expected structure of (tetramer). A complete NMR spectral analysis was not possible because of the presence of multiple near-equivalent conformers and slight (but symmetry-breaking) *cis-trans* isomerization at proline 9.

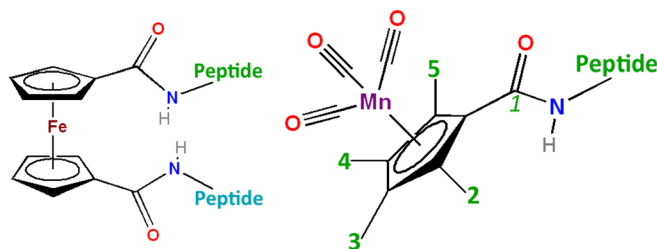


Figure 15. Ferrocene and cymantrene peptides. Isomers with methyl groups in the 2, 3, 4, and 5 positions were investigated (these positions are inequivalent as part of a chiral captide). In terms of synthesis, the carboxylic acid group was added to the existing methyl cymantrene (ferrocene dicarboxylic acid was commercially available).

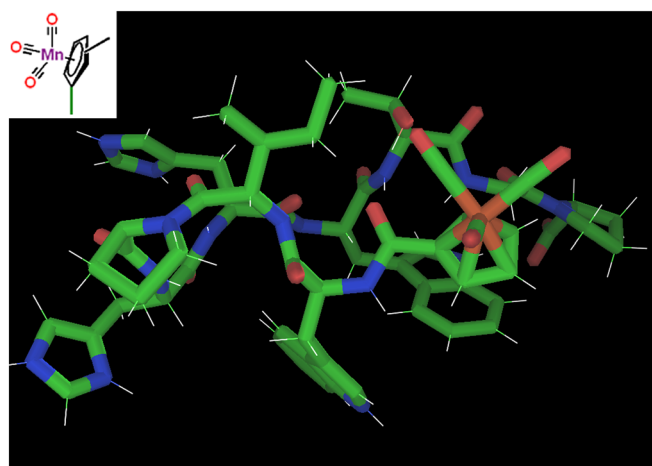


Figure 16. Cymantrene captide model, verified by NOEs for the variants with a methyl group at 3 position or 4 position (clashes occur at 5 and especially 2 positions, as supported by the lower fold populations we observe via NMR). Note close contacts between Ile2/Thr7 and a CO ligand. A lysine or arginine at these positions could reach to the inner coordination sphere of the metal site.

For this study, we chose to carboxylate methyl cymantrene at its four inequivalent aromatic positions, for two reasons: (i) to gain structural information regarding the resulting non-equivalent *ortho* positions and (ii) because methyl cymantrene is an inexpensive commodity chemical due to its use as an anti-knock additive in gasoline and therefore more relevant for the study. Methyl cymantrene (methyl-cyclopentadienyl manganese tricarbonyl) was carboxylated according to the method of Biehl and Reeves [37,38].

Three of the four methyl cymantrene captides were well folded. Isomers 3 and 4 (methyl groups in positions *meta* to amide 1) were similar: both adopted the very stable ($\chi_F = 0.98$) captide structure. Conversely, the 2-isomer and 5-isomer differed significantly; isomer 2 (amide proton toward methyl) was significantly less stable than isomer 5 (χ_F 's of 0.72 and 0.86, respectively).

Although the lack of hydrogens on the CO ligands precluded direct detection, models suggest close contact between the CO ligands and the peptide sidechains – most notably Ile2 and Thr7, which are amenable to mutation. This recommends our captide constructs as ideal springboards to hybrid peptide/small molecule catalysts: small constructs with precise, chiral, active site-like control over the local environment.

Metal-binding hubs

Potential catalysts are not limited to cyclopentadienyl-containing systems. The mono-chain and di-chain WlpKKWTGP-NH₂ adducts of a number of metal-binding small molecules were shown to adopt the expected stable captide structures. Dicarboxylic acids of 2,2'-bipyridine (carboxyl groups attached at both 4,4'-position and 5,5'-position), 2,9 phenanthroline di-carboxylic acid, two isomers of 8-hydroxyquinoline, and the aforementioned dipicolinic acid [51] were among the metal-binding small molecule hubs investigated. Peptide adducts of these metal-binding systems have been examined previously, but the peptides employed were unstructured entities [51–56].

These constructs display less avid metal binding than might have been expected, likely because metal binding results in higher-order assemblies. It should be noted that polycationic peptides have been known to abolish (or at least seriously hinder) iron II – bipyridine binding and the formation of a tris-Bpy core [56], otherwise, a very rapid, favorable, and easily characterizable process. This is especially true in our case as any D3-symmetric hexamer of our bipyridine captides would be expected to have very serious steric clashes. The peptide chains could not remain folded on Fe II binding; hence, poor Fe II affinities and solubility difficulties were observed.

Other applications of captides

While catalysis may require significant modeling and experimental testing, other applications of captide constructs are more straightforward. For example, small molecules with orthogonal reactivity allow for higher-order assembly without any need for metals. With this in mind, we validated the captide structure and stability of adducts of polymer-forming propionic, acrylic, methacrylic, and 2-bromothiophene-5-carboxylic acid. Although attaching these compounds to peptides is not inherently novel, the structured environment of captide scaffolds is expected to alter reactivity of these monomers and impart new properties to resulting polymers; for example, acrylic captide should theoretically polymerize to a hydrophilic polyacrylamide chain fully buried by crowded beta hairpin units.

Our proof-of-concept work extended to fluorophores as well: methyl red, DABCYL, and fluorescein resulted in well-folded captide constructs, as expected. We are currently exploring a niche application for determining Förster Resonance Energy Transfer (FRET) pair efficiency calibration between two probes at precise distances and angles; there is a distinct advantage over calibration techniques using intervening proline units [57].

Captides from longer β -capped peptide structures

To increase the range of validated uses for this captide technology and verify its general applicability to beta sheets of any topology, we investigated longer beta sheet/small molecule adducts. Although the small captide test system is sufficient for most applications, the usefulness of this technology stems from the ability to set any small molecule at the end of any structured beta sheet peptide. Thus, we attached a longer capped hairpin to ferrocene dicarboxylic acid, forming a two-chain dimer analogous to the short captide test case heretofore explored. This longer hairpin, WITVTIHGKKIRVWTG-NH₂, was previously shown to be >98% folded by H/D exchange, as the N-acetyl adduct [33]. CSDs matched those of the acetylated monomer almost exactly, suggesting that individual chains adopted the expected hairpin structure. The only difference was somewhat broader

resonances in the case of the ferrocene adduct. The expected structure is shown in Figure 17.

Disulfide-dimerized captides

Another application of captide-like species is positioning two singly bound small molecules at the ends of a rigid dimeric beta sheet. These ‘two-headed’ twice beta-capped systems are exceptionally stable disulfide-bound C2-symmetric homodimers; they effectively replace the beta turn portion of a hairpin with another Trp/Trp beta cap [33] (see Figure 18 for an example). To confirm that N-terminal carboxylic attachments larger than acetyl are viable in this context, we investigated oxidized WHTHCIRTWTGP-NH₂ with a p-iodobenzoyl group bound to its N-terminus; a model appears in Figure 18. This peptide formed a C2-symmetric dimer with all the expected β -capped sheet diagnostics in place, in addition to chemical shifts of the intervening chain(s) that suggested a fully folded ($\chi_F > 0.96$) β -sheet.

These two-headed constructs open up more potential applications: multi-electron transfer via two precisely spaced one-electron redox agents, higher-order assembly (assuming that precisely correct angles can be established), multivalent drugs, and so on. The β -sheets can be of various lengths: we have validated β -sheets of 5, 9, and 13 amino acid strand length, and longer sheets should be viable as well. Rigid linkers can be optimized to span membranes or bridge two binding sites. And because hetero-constructs can be synthesized with only 50% yield penalty, two small molecules can be held at

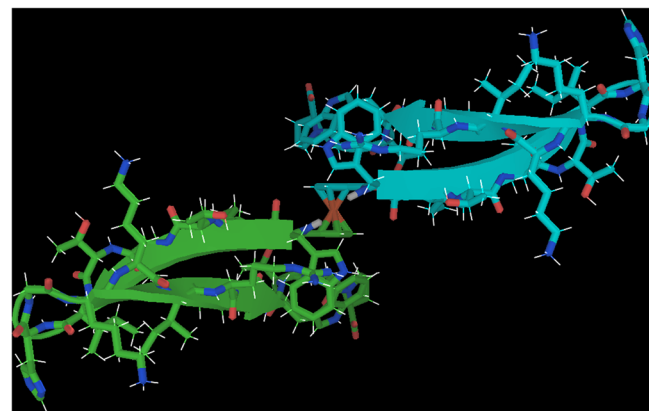


Figure 17. Ferrocene-hub dimer of WITVTIHGKKIRVWTG-NH₂. Intrachain structure was readily confirmed by NOEs and CSDs, but interchain contacts were more ambiguous because of line broadening near the hub.

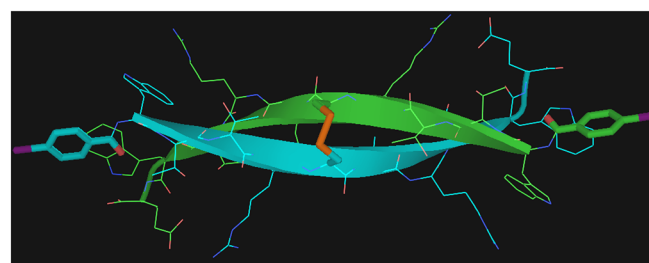


Figure 18. NOE-validated model of a stable beta sheet dimer. The functionalizable end groups are set at specific angles and distances, which can be modulated by the length of the central beta sheet.

specific distances and with specific orientations; this should prove to be an optimal system for FRET and electron transfer calibration studies.

Conclusion

Although chemical modification of peptides is by no means new, captides (rigidly oriented β -capped peptide/small molecule adducts with the small molecule carboxyl serving as a keystone required for peptide folding) represent a novel technology with a multitude of potential applications. In this proof-of-concept study, we have determined that a wide range of small molecules can be given a specific peptide context using a nine-residue peptide unit. We have elucidated how the adducted small molecules orient themselves in relation to the hairpin peptide and how they alter (or in most cases, do not alter) its structure.

This study is, in part, a response to the lamentable nearly ubiquitous use of long flexible linkers such as PEGs for current peptide/small molecule conjugation. We have, in contrast, highly structured constructs. In cases where the specific captide structure is not always ideal (e.g., it causes greatly reduced metal binding), it can be modified via mutations of some sidechains and/or placed in other beta sheet terminating contexts. Moving forward, we seek to thoroughly investigate some specific possibilities we have hinted at here. We will also seek crystal structure data; our NMR data is clear, but we want atomistic confirmations for especially structure-sensitive applications such as catalysis. The design of chiral catalysts based on captides is a high priority goal.

Acknowledgement

This work was supported in large part by the National Institutes of Health (NIH) Grant GM099889 (Niels H. Andersen, P.I.).

References

1. Falciani C, Lozzi L, Pini A, Corti F, Fabbrini M, Bernini A, Lelli B, Niccolai N, Bracci L. Molecular basis of branched peptides resistance to enzyme proteolysis. *Chem. Biol. Drug Des.* 2007; **69**: 216–221.
2. Bird GH, Madani N, Perry AF, Princiotti AM, Supko JG, He X, Gavathiotis E, Sodroski JG, Walensky LD. Hydrocarbon double-stapling remedies the proteolytic instability of a lengthy peptide therapeutic. *Proc. Natl. Acad. Sci. U. S. A.* 2010; **107**: 14093–14098.
3. Arnesen T. Towards a functional understanding of protein N-terminal acetylation. *PLoS Biol.* 2011; **9**: 5.
4. Koehler MFT, Zobel K, Beresini MH, Caris LD, Combs D, Paasch BD, Lazarus RA albumin affinity tags increase peptide half-life in vivo. *Bioorg. Med. Chem. Lett.* 2002; **12**: 2883–2886.
5. Jones AT, Sayers EJ. cell entry of cell penetrating peptides: tales of tails wagging dogs. *J. Control. Release* 2012; **161**: 582–591.
6. Al-Ahmady ZS, Al-Jamal WT, Bossche JV, Bui TT, Drake AF, Mason AJ, Kostarelos K. Lipid-peptide vesicle nanoscale hybrids for triggered drug release by mild hyperthermia in vitro and in vivo. *ACS Nano* 2012; **6**: 9335–9346.
7. Weinstain R, Savariar EN, Felsen CN, Tsien RY. In vivo targeting of hydrogen peroxide by activatable cell-penetrating peptides. *J. Am. Chem. Soc.* 2014; **136**: 874–877.
8. Soler M, Gonzalez M, Soriano-Castell D, Ribas X, Costas M, Tebar F, Massagué A, Feliz L, Planas M. Identification of BP16 as a non-toxic cell-penetrating peptide with highly efficient drug delivery properties. *Org. Biomol. Chem.* 2014; **12**: 1652–1663.
9. Yagi N, Yano Y, Hatanaka K, Yokoyama Y, Okuno H. Synthesis and evaluation of a novel lipid-peptide conjugate for functionalized liposome. *Bioorg. Med. Chem. Lett.* 2007; **17**: 2590–2593.
10. Reback ML, Buchko GW, Kier BL, Ginovska-Pangovska B, Xiong Y, Hou J, Roberts JAS, Sorensen CM, Raugei S, Squier TC, Shaw WJ. Enzyme design from the bottom up: an active nickel electrocatalyst with a structured peptide outer coordination sphere. *Chem. Eur. J.* 2014; **20**: 1510–1514.
11. Ippoliti R, Picciu A, Santucci R, Antonini G, Brunori M, Ranghino G. Microperoxidase: covalent complex of microperoxidase with a 21-residue synthetic peptide as a mequette for low-molecular-mass redox proteins. *Biochem. J.* 1997; **328**: 833–840.
12. Ni TW, Tezcan FA. Structural characterization of a microperoxidase inside a metal-directed protein cage. *Angew. Chem. Int. Ed. Engl.* 2010; **49**: 7014–7018.
13. Brûlé E, Hii KK, de Miguel YR. Polymer-supported manganese porphyrin catalysts – peptide-linker promoted chemoselectivity. *Org. Biomol. Chem.* 2005; **3**: 1971–1976.
14. Li S, Roberts RW. A novel strategy for in vitro selection of peptide-drug conjugates. *Chem. Biol.* 2003; **10**: 233–239.
15. Reddy MM, Bachhawat-Sikder K, Kodadek T. Transformation of low-affinity lead compounds into high-affinity protein capture agents. *Chem. Biol.* 2004; **11**: 1127–1137.
16. Pessi A, Langella A, Capitò E, Ghezzi S, Vicenzi E, Poli G, Ketts T, Mathieu C, Cortese R, Horvat B, Moscona A, Porotto M. A general strategy to endow natural fusion-protein-derived peptides with potent antiviral activity. *PLoS One* 2012; **7**: e36833.
17. Vadehra GS, Wall BD, Diegelmann SR, Tovar JD. On-resin dimerization incorporates a diverse array of pi-conjugated functions in aqueous assembling peptides. *Chem. Commun.* 2010; **46**: 3947–3949.
18. Wall BD, Tovar JD. Synthesis and characterization of pi-conjugated peptide-based supramolecular materials. *Pure Appl. Chem.* 2012; **84**: 1039–1045.
19. Gutiérrez-Abad R, Illa O, Ortúñoz RM. Synthesis and structure of chiral cyclobutane containing C3-symmetric peptide dendrimers. *Org. Lett.* 2010; **12**: 3148–3151.
20. Sakaguchi K, Kodama H, Matsumoto H, Yoshida M, Takano Y, Kamiya H, Waki M, Shimohigashi Y. Design and synthesis of dimeric analogs of neurokinin A and B: effect of dimerization of COOH-terminal heptapeptides on receptor selection. *Pept. Res.* 1989; **5**: 345–351.
21. Pillai R, Marinelli ER, Swenson RE. A flexible method for preparation of peptide homo- and heterodimers functionalized with affinity probes, chelating ligands, and latent conjugating groups. *Biopol. Pept. Sci.* 2006; **84**: 576–585.
22. Johnson DL, Farrell FX, Barbone FP, McMahon FJ, Tullai J, Kroon D, Freedy J, Zivin RA, Mulcahy LS, Jolliffe LK. Amino-terminal dimerization of an erythropoietin mimetic peptide results in increased erythropoietic activity. *Chem. Biol.* 1997; **4**: 939–950.
23. Xiao J, Hamilton BS, Tolbert TJ. Synthesis of N-terminally linked protein and peptide dimers by native chemical ligation. *Bioconjug. Chem.* 2010; **21**: 1943–1947.
24. Tam JP, Zavala F. Multiple antigen peptide. A novel approach to increase detection sensitivity of synthetic peptides in solid-phase immunoassays. *J. Immunol. Methods* 1989; **124**: 53–61.
25. Kowalczyk W, Monsó M, de la Torre BG, Andreu D. Synthesis of multiple antigenic peptides MAPs – strategies and limitations. *J. Pept. Sci.* 2011; **17**: 247–251.
26. Crespo L, Sanclimens G, Pons M, Giralt E, Royo M, Albericio F. Peptide and amide-bond containing dendrimers. *Chem. Rev.* 2005; **105**: 1663–1681.
27. Zhao Y, Imura T, Leman LJ, Curtiss LK, Maryanoff BE, Ghadiri MR. Mimicry of high-density lipoprotein: functional peptide-lipid nanoparticles based on multivalent peptide constructs. *J. Am. Chem. Soc.* 2013; **135**: 13414–13424.
28. Kok WM, Scanlon DB, Karas JA, Miles LA, Tew DJ, Parker MW, Barnham KJ, Hutton CA. Solid-phase synthesis of homodimeric peptides: preparation of covalently-linked dimers of amyloid b peptide. *Chem. Commun.* 2009; **41**: 6228–6230.
29. Salgado EN, Brodin JD, To MM, Tezcan FA. Templated construction of a Zn-selective protein dimerization motif. *Inorg. Chem.* 2011; **13**: 6323–6329.
30. Reback ML, Ginovska-Pangovska MSB, Ho M-H, Jain A, Squier TC, Raugei S, Roberts JAS, Shaw WJ. The role of a dipeptide outer-coordination sphere on H₂-production catalysts: influence on catalytic rates and electron transfer. *Chem. Eur. J.* 2013; **19**: 1928–1941.
31. Jain A, Buchko GW, Reback ML, O'Hagan M, Ginovska-Pangovska B, Linehan JC, Shaw WJ. Active hydrogenation catalyst with a structured, peptide-based outer-coordination sphere. *ACS Catal.* 2012; **2**: 2114–2118.

32. Monney A, Nastri F, Albrecht M. Peptide-tethered monodentate and chelating histidylidene metal complexes: synthesis and application in catalytic hydrosilylation. *Dalton Trans.* 2013; **42**: 5655–5660.
33. Kier BL, Shu I, Eidenschink LA, Andersen NH. Stabilizing capping motif for beta hairpins and sheets. *Proc. Natl. Acad. Sci. U. S. A.* 2010; **107**: 10466–10471.
34. Kier BL, Andersen NH. Probing the lower size limit for protein-like fold stability: ten-residue microproteins with specific, rigid structures in water. *J. Am. Chem. Soc.* 2008; **130**: 14675–14683.
35. Cochran AG, Skelton NJ, Starovasnik MA. Tryptophan zippers: stable, monomeric beta-hairpins. *Proc. Natl. Acad. Sci. U. S. A.* 2001; **98**: 5578–5583.
36. Fesinmeyer RM, Hudson FM, Andersen NH. Enhanced hairpin stability through loop design: the case of the protein G B1 domain hairpin. *J. Am. Chem. Soc.* 2004; **126**: 7238–7243.
37. Biehl ER, Reeves PC. A convenient, high-yield synthesis of the carboxylic acid derivatives of ferrocene and cyclopentadienylmanganese tricarbonyl. *Synthesis* 1973; 360–361.
38. Reeves PC. Carboxylation of aromatic compounds: ferrocene-carboxylic acid. *Org. Synth.* 1977; **56**: 28.
39. Eidenschink LA, Kier BL, Huggins KNL, Andersen NH. Very Short peptides with stable folds: building on the interrelationship of Trp/Trp, Trp/cation, and Trp/backbone-amide interaction geometries. *Protein Struct. Funct. Bioinf.* 2009; **75**: 308–322.
40. Scian M, Shu I, Olsen KA, Hassam K, Andersen NH. Mutational effects on the folding dynamics of a minimized hairpin. *Biochemistry* 2013; **52**: 2556–2564.
41. Olsen KA, Fesinmeyer RM, Stewart JM, Andersen NH. Hairpin folding rates reflect mutations within and remote from the turn region. *Proc. Natl. Acad. Sci. U. S. A.* 2005; **102**: 15483–15487.
42. Andersen NH, Olsen KA, Fesinmeyer RM, Tan X, Hudson FM, Eidenschink LA, Farazi SR. Minimization and optimization of designed beta-hairpin folds. *J. Am. Chem. Soc.* 2006; **128**: 6101–6110.
43. Blake CCF. Small RWH The crystal structure of benzamide. *Acta Crystallogr. B* 1972; **28**: 2201.
44. Fong CW, Grant HG. Torsional angles in N-substituted benzamides and related compounds by carbon-13 N.M.R. Chemical shifts. *Aust. J. Chem.* 1981; **34**: 957–967.
45. Prabhakaran P, Azzarito V, Jacobs T, Hardie MJ, Kilner CA, Edwards TA, Warriner SL, Wilson AJ. Conformational properties of O-alkylated benzamides. *Tetrahedron* 2012; **68**: 4485–4491.
46. Elschenbroich C, Salzer A. Overview of Cp^{*} Compounds. From *Organometallics: a Concise Introduction*, 1989; p. 47
47. Spradau TW, Katzenellenbogen JA. Protein and peptide labeling with cyclopentadienyltricarbonyl rhenium and technetium. *Bioconjug. Chem.* 1998; **9**: 765–772.
48. Splitk K, Neundorf I, Hu W, N'Dongo HWP, Vaslyeva V, Merz K, Schatzschneider U. Influence of the metal complex-to-peptide linker on the synthetic properties of bioactive CpMnCO₃ peptide conjugates. *Dalton Trans.* 2010; **39**: 2536–2545.
49. Splitk K, Hu W, Schatzschneider U, Gust R, Ott I, Onambale LA, Prokop A, Neundorf I. Protease-activatable organometal-peptide bioconjugates with enhanced cytotoxicity on cancer cells. *Bioconjug. Chem.* 2010; **21**: 1288–1296.
50. Nadeem Q, Can D, Shen Y, Felber M, Mahmood Z, Alberto R. Synthesis of tripeptide derivatized cyclopentadienyl complexes of technetium and rhenium as radiopharmaceutical probes. *Org. Biomol. Chem.* 2014; **12**: 1966–1974.
51. Moriuchi T, Morimoto K, Sakamoto Y, Hirao T. Molecular structures of dipeptide-palladium(II) conjugated complexes. *Eur. J. Inorg. Chem.* 2012; **29**: 4669.
52. Pilz CS, Steinem C. Modulation of the conductance of a 2,2'-bipyridine-functionalized peptidic ion channel by Ni²⁺. *Biophys. Lett.* 2008; **37**: 1065–1071.
53. Ogawa M, Balan B, Ajayakumar G, Masaoka S, Kraatz HB, Muramatsu M, Ito S, Nagasawa Y, Miyasaka H, Sakai K. Photoinduced electron transfer in tris2,2'-bipyridineruthenium(II)-viologen dyads with peptide backbones leading to long-lived charge separation and hydrogen evolution. *Dalton Trans.* 2010; **39**: 4421–4434.
54. Lee SK, Yoon SS. Syntheses and peptide-binding properties of metal-templated self-assembly. *Bull. Korean Chem. Soc.* 2008; **29**: 234–236.
55. Bishop BM, McCafferty DG, Erickson DW. 4'-Aminomethyl-2,2'-bipyridyl-4-carboxylic acid Abc and Related derivatives: novel bipyridine amino acids for the solid-phase incorporation of a metal coordination site within a peptide backbone. *Tetrahedron* 2000; **56**: 4629–4638.
56. Uhlich NA, Sommer P, Bühr C, Schürch S, Reymond J-L, Darbre T. Remote control of bipyridine–metal coordination within a peptide dendrimer. *Chem. Commun.* 2009; 6237–6239.
57. Schuler B, Lipman EA, Steinbach PJ, Kumke M, Eaton WA. Polyproline and the “spectroscopic ruler” revisited with single-molecule fluorescence. *Proc. Natl. Acad. Sci. U. S. A.* 2004; **102**: 2754–2759.

Supporting Information

Additional supporting information may be found in the online version of this article at the publisher's web site.